# A Nipkow disk integrated with Fresnel lenses for terahertz single pixel imaging

**Chong Li,* James Grant, Jue Wang, and David R. S. Cumming**

*School of Engineering, University of Glasgow, Glasgow, G12 8LT, UK*
*chong.li@glasgow.ac.uk*

**Abstract:** We present a novel Nipkow disk design for terahertz (THz) single pixel imaging applications. A 100 mm high resistivity (ρ≈3k-10k Ω·cm) silicon wafer was used for the disk on which a spiral array of twelve 16-level binary Fresnel lenses were fabricated using photolithography and a dry-etch process. The implementation of Fresnel lenses on the Nipkow disk increases the THz signal transmission compared to the conventional pinhole-based Nipkow disk by more than 12 times thus a THz source with lower power or a THz detector with lower detectivity can be used. Due to the focusing capability of the lenses, a pixel resolution better than 0.5 mm is in principle achievable. To demonstrate the concept, a single pixel imaging system operating at 2.52 THz is described.



**OCIS codes:** (110.0110) Imaging systems; (110.67952700) Terahertz imaging; (050.0050) Diffraction and gratings; (050.1965) Diffractive lenses.

## References and links

1. Y. C. Shen, T. Lo, P. F. Taday, B. E. Cole, W. R. Tribe, and M. C. Kemp, "Detection and identification of explosives using terahertz pulsed spectroscopic imaging," Appl. Phys. Lett. **86**(24), 24116 (2005).
2. J. B. Jackson, M. Mourou, J. F. Whitaker, I. N. Duling III, S. L. Williamson, M. Menu, and G. A. Mourou, "Terahertz imaging for non-destructive evaluation of mural paintings," Opt. Commun. **281**(4), 527–532 (2008).
3. P. H. Siegel, "Terahertz technology in biology and medicine," IEEE Trans. Microw. Theory Tech. **52**(10), 2438–2447 (2004).
4. A. Dobroiu, M. Yamashita, Y. N. Ohshima, Y. Morita, C. Otani, and K. Kawase, "Terahertz imaging system based on a backward-wave oscillator," Appl. Opt. **43**(30), 5637–5646 (2004).
5. T. Yasuda, Y. Kawada, H. Toyoda, and H. Takahashi, "Terahertz movie of internal transmission imaging," Opt. Express **15**(23), 15583–15588 (2007).
6. B. B. Hu and M. C. Nuss, "Imaging with terahertz waves," Opt. Lett. **20**(16), 1716–1718 (1995).
7. A. Nahata, J. T. Yardley, and T. F. Heinz, "Two-dimensional imaging of continuous-wave terahertz radiation using electro-optic detection," Appl. Phys. Lett. **81**(6), 938–963 (2002).
8. W. L. Chan, K. Charan, D. Takhar, K. F. Kelly, R. G. Baraniuk, and D. M. Mittleman, "A single-pixel terzhertz imaging system based on compressed sensing," Appl. Phys. Lett. **93**(12), 121105 (2008).
9. A. W. Lee and Q. Hu, "Real-time, continuous-wave terahertz imaging by use of a microbolometer focal-plane array," Opt. Lett. **30**(19), 2563–2565 (2005).
10. J. Yang, S. Ruan, and M. Zhang, "Real-time, continuous-wave terahertz imaging by a pyroelectric camera," Chin. Opt. Lett. **6**(1), 29–31 (2008).
11. A. W. Lee, Q. Qin, S. Kumar, B. S. Williams, Q. Hu, and J. L. Reno, "Real-time terahertz imaging over a standoff distance (> 25 meters)," Appl. Phys. Lett. **89**(14), 141125 (2006).
12. F. Schuster, D. Coquillat, H. Videlier, M. Sakowicz, F. Teppe, L. Dussopt, B. Giffard, T. Skotnicki, and W. Knap, "Broadband terahertz imaging with highly sensitive silicon CMOS detectors," Opt. Express **19**(8), 7827–7832 (2011).
13. J. Baird, "Apparatus for transmitting views or images to a distance" patent, US1699270, January 1929.
14. M. D. Egger and M. Petrăn, "New reflected-light microscope for viewing unstained brain and ganglion cells," Science **157**(3786), 305–307 (1967).
15. G. Q. Xiao, T. R. Corle, and G. S. Kino, "Real-time confocal scanning optical microscope," Appl. Phys. Lett. **53**(8), 716–718 (1988).
16. J. W. Lichtman, W. J. Sunderland, and R. S. Wilkinson, "High-resolution imaging of synaptic structure with a simple confocal microscope," New Biol. **1**(1), 75–82 (1989).
17. T. Tanaami and K. Mikuriya, "Nipkow disk for confocal optical scanner" European Patent Office, EP0539691 A2, 5 May 1993.
18. R. Gräf, J. Rietdorf, and T. Zimmermann, "Live cell spinning disk microscopy," Adv. Biochem. Eng. Biotechnol. **95**, 57–75 (2005).

#193636 - $15.00 USD Received 9 Jul 2013; revised 12 Sep 2013; accepted 24 Sep 2013; published 7 Oct 2013

19. Y. Takahara, N. Matsuki, and Y. Ikegaya, "Nipkow confocal imaging from deep brain tissues," J. Integr. Neurosci. **10**(01), 121–129 (2011).
20. Y. Ma, J. Grant, S. Saha, and D. R. S. Cumming, "Terahertz single pixel imaging based on a Nipkow disk," Opt. Lett. **37**(9), 1484–1486 (2012).
21. E. Hecht, *Optics* 4th Edition, (Addison Wesley, 2001).
22. M. B. Stern, "Binary optics: A VLSI-based microptics technology," Microelectron. Eng. **32**(1-4), 369–388 (1996).
23. E. D. Walsby, S. Wang, J. Xu, T. Yuan, R. Blaikie, S. M. Durbin, X.-C. Zhang, and D. R. S. Cumming, "Multilevel silicon diffractive optics for terahertz waves," J. Vac. Sci. Technol. **20**(6), 2780–2783 (2002).
24. S. C. Saha, C. Li, Y. Ma, J. P. Grant, and D. R. S. Cumming, "Fabrication of multilevel silicon diffractive lens at terahertz frequency," IEEE Trans. Terahertz Sci. Tech. **3**(4), 479–485 (2013).
25. M. S. Alam, J. G. Bognar, R. C. Hardie, and B. J. Yasuda, "Infrared image registration and high-resolution reconstruction using multiple translationally shifted aliased video frames," IEEE Trans. Instrum. Sci. Technol. **49**(5), 915–923 (2000).

## 1. Introduction

Terahertz (THz) imaging systems have recently received extensive attention among researchers for applications in the fields of security screening, non-invasive inspection and spectroscopy [1–12], as a consequence of the unique properties of electromagnetic waves in the THz frequency range 0.1 THz-30 THz. Terahertz radiation is non-ionising, transmits through fabrics and plastics and is strongly absorbed by water. THz imaging systems can be categorized into single detector [6–8] and multi or array detector imaging systems [9–12]. The former, using pyroelectric devices, Golay cells or Schottky diodes, has the advantage of low cost and high resolution. As an alternative, array detector based imaging systems using bolometers typically require far less time to construct a THz image [9, 11]. Nevertheless, THz imaging systems based on single detector technology is currently the main stream in commercial products for scientific research.

In conventional optical single detector imaging systems, translation stages are commonly used to move either the object or detector to achieve the mechanical scanning [6–8]. Nipkow disks have also been used to achieve relatively faster scanning speeds and have been influential in imaging technology for many years, including the early development of television [13]. However, because of low light transmission, limited by the pinhole size, the technique was abandoned for many decades. In 1967, when multiple threads of spiral pinholes were published by Egger and Petran [14], Nipkow disks gained new attention. The Archimedean spiral pinholes accommodated many thousands of pinholes and improved the light transmission by multiplexing illumination. However, the imaging setup was very complicated. Although improvements were made by Kino and Lichtman in the late 1980s [15, 16], the transmission efficiency was still low. In 1991, Tanaami and Mikuriya presented a new design of Nipkow disk that integrated microlenses and demonstrated improved transmission of up to 1000 times [17]. Nipkow disks are still used in modern microscopy [18, 19].

For THz single detector imaging systems, the scanning technique that is used in many systems is based on translation stages or rotating mirrors. Recently, Ma et al demonstrated a Nipkow based single pixel imaging system at 2.52 THz [20]. The system, using a conventional disk with pinholes, resulted in an approximate axial resolution of 2 mm/pixel using a simple scan. Although smaller pinholes could be used to further improve the resolution, the transmitted power would have been reduced. Thus, detectors with high detectivity and sensitivity or sources with high emission power, which are currently scarce at THz frequencies, are required. In this paper, we present a new design of Nipkow disk for a THz single pixel imaging system. Similar to the Nipkow disk developed by Tanaami and Mikuriya for optical imaging systems, we demonstrate a Nipkow disk of terahertz lenses. Unlike Tanaami and Mikuriya we use a silicon wafer on which multiple THz diffractive lenses (Fresnel lenses) are fabricated in order to simplify manufacture and produce a precision lightweight structure. The design gives more than 12 times higher power transmission compared to pinhole-based Nipkow disks so that an imaging system built with the disk can use a weaker power source or a detector with lower detectivity. The imaging system that we describe is mechanically simple to build and provides a fully sampled raster-

#193636 - $15.00 USD Received 9 Jul 2013; revised 12 Sep 2013; accepted 24 Sep 2013; published 7 Oct 2013

scanned frame. Unlike compressed imaging [8] there is no need for software reconstruction of the image. We will first describe the design, fabrication and characterization of the Nipkow disk, and then an imaging system that uses the disk with a 2.52 THz laser and a single pixel pyroelectric detector.

## 2. Disk design, fabrication and characterization

For a conventional Nipkow disk with a single spiral pinhole array as shown in Fig. 1(a) [20], the size of the imaging area in the radial direction is determined by the product of the number of pinholes, $N$, and the radial separation between two pinholes, $\Delta l$, i.e. $l1$-$l2$ in Fig. 1(a). On the other hand, the size of the imaging area in the rotational direction is then determined by the sectorial distance between two pinholes. The resolution of the imaging system is then determined by the size of the pinhole, the rotational speed of the disk, and the response time of the detector. Resolution is also limited by diffraction from the pinholes in the disk. The irradiance, $I_0$, at a point P on the central axis of the pinhole at a distance of $R$ is determined by

$$I_0 = \frac{\varepsilon_A^2 A^2}{2R^2} \tag{1}$$

where $A$ is the pinhole area and $\varepsilon_A$ is the source strength per unit area [21]. Since the pinhole size affects the radial separation between two adjacent pinholes, hence the limit of image resolution, smaller diameter pinholes are required for a higher resolution image, but at the expense of greater loss of signal in the system. According to Eq. (1), smaller diameter pinholes allow less power transmission through the pinhole, thus reducing the signal at the imaging plane and therefore the received power at the detector. To achieve similar image quality a stronger signal source providing higher $\varepsilon_A$ or a more sensitive detector with higher detectivity is required.

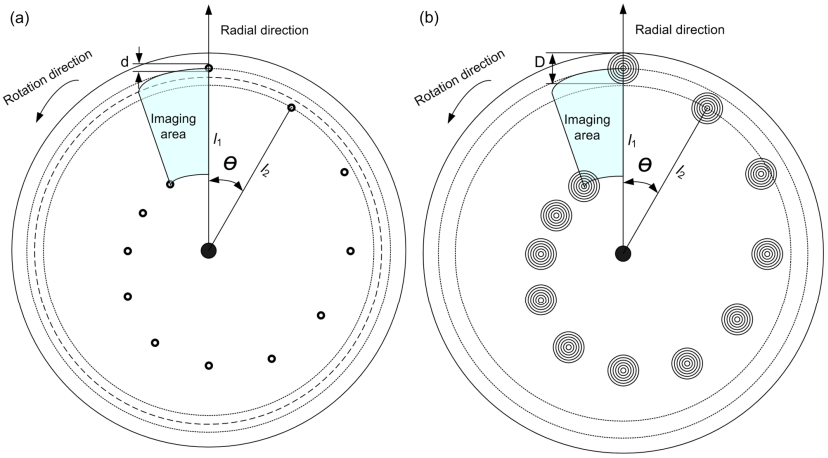


Fig. 1. Illustration of the conventional and proposed Nipkow disks. (a) A conventional Nipkow disk with single spiral pinhole array. (b) The proposed Nipkow disk with THz Fresnel lens array.

An alternative solution is to capture more of the available signal and direct the power on to the detector [21]. A suitable method of achieving this is to integrate microlenses on to the Nipkow disk itself. To do so, we used a 4-inch (100 mm) diameter double-side polished high resistivity (approximately 3-10 kΩ•cm) silicon wafer as disk into which the lenses are directly fabricated. The unmodified wafer has a thickness of 325 μm and a transmittance of 50%-60% at terahertz frequencies. A binary fabrication technique was used to develop the lenses on the silicon wafer [22–24]. Constrained by the size of the silicon wafer, 12 Fresnel lenses having a diameter of 10 mm were arranged spirally with an axial separation of 2 mm. Figure 1(b) illustrates the design layout of the proposed disk.

#193636 - $15.00 USD Received 9 Jul 2013; revised 12 Sep 2013; accepted 24 Sep 2013; published 7 Oct 2013

The maximum radius, $R_n$, and the focal length, $f$, were chosen to be 5 mm and 55 mm, respectively. This leads the number of zones, $n$, to be 2 [23]. Since a binary photolithography fabrication technique was used to make the lenses, the number of photo masks, $k$, determines the number of phase steps, $m$ ($m = 2^k$). Thus, the radius of each phase step, $R_{ni}$, can be calculated from [23, 24]

$$R_{ni} = \sqrt{\lambda f(2\frac{i}{m} + 2n - 2)} \tag{2}$$

where $\lambda$ is the wavelength at the specific frequency, that is 119 μm for our design at 2.5 THz and $i$ represents each individual phase step. The total etch depth, $h$, for silicon, with a refractive index of 3.42, is 49 μm [23]. Table 1 summarises all the design parameters for a binary diffractive lens with a diameter of 10 mm and focal length of 55 mm on a 4-inch double-side polished silicon wafer.

**Table 1. Parameters for the Design of a Silicon Wafer Based Nipkow Disk with Integration of Diffractive Lenses**

| Symbol | Description | Value |
|---|---|---|
| $\lambda$ | Wavelength at the central design frequency of 2.5 THz | 119 μm |
| $D$ | Diameter of Fresnel lens | 10 mm |
| $h$ | Total etch depth | 49 μm |
| $\eta$ | Refractive index of silicon | 3.42 |
| $n$ | Number of zones | 2 |
| $f$ | Focal length of the lens | 55 mm |
| $m$ | Total numbers of steps | 16 |
| $N$ | Number of lenses | 12 |
| $\Delta l$ | Distance between centers of two adjacent lenses | 2 mm |

The disk fabrication used in this work is similar to the 4-mask 16-level binary silicon diffractive lens fabrication process described in [24] except an additional layer of alignment markers was made before commencing the subsequent photolithography and dry-etch processes. The alignment markers were fabricated using electron beam lithography and a metal lift-off process. Electron beam lithography allows flexible prototyping and ensures precise alignment and overlay using the marker patterns on the disk during fabrication. Two layers of polymethylmethacrylate (PMMA) with a concentration of 15% and 4% in ethyl lactate were used as a positive electron beam resist. A Vistec VB6 was used for pattern writing. A 10 nm/100 nm Ti/Au metal stack was deposited after the sample was developed in IPA:MIBK 1:1 and then put in acetone for metal lift-off. Once the markers were defined the 4-mask Fresnel lens fabrication process was followed, as described in detail in [24], to achieve 16 level binary diffractive lenses. An optical image of the completed disk is shown in Fig. 2.

Figure 3(a) shows the measured typical surface profile of the fabricated Fresnel lenses using a Dektak profilometer with a 2.5 μm radius stylus and 7 mg force. One can see there is good alignment of the 4 lithography layers. An SEM image at the central cut-off plane was later taken by using Hitachi S4700 and is also shown in Fig. 3(b).

#193636 - $15.00 USD Received 9 Jul 2013; revised 12 Sep 2013; accepted 24 Sep 2013; published 7 Oct 2013

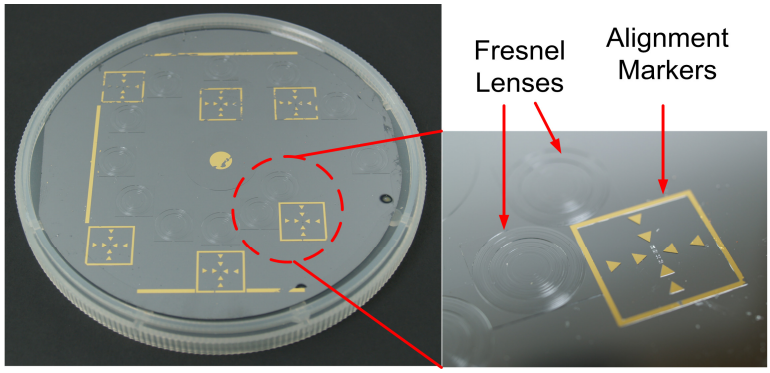


Fig. 2. Optical image of the fabricated THz silicon Nipkow disk with integration of twelve 16-level binary diffractive lenses.

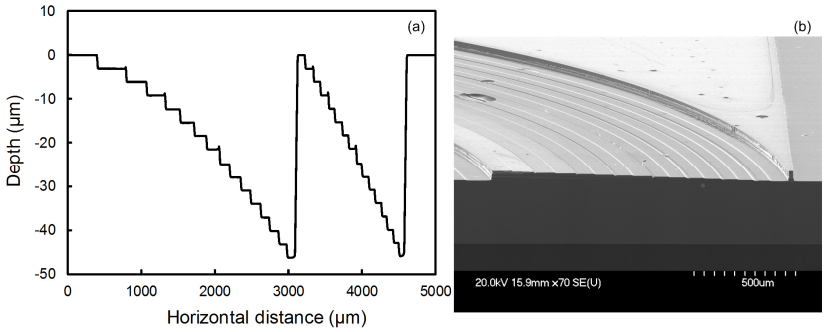


Fig. 3. (a) Surface profile of a typical Fresnel lens and (b) an SEM image of a lens at the central cut-off plane.

The focal length and size of the beam disk diameter at the focal point of each lens were characterised using a $CO_2$ laser pumped methanol vapour THz laser (Edinburgh Instruments) operating at 2.52 THz and an IR focal plane array (FPA, Photon 320). The experimental setup is shown in Fig. 4(a). An image of the focal spot of one of the lenses taken using the IR camera at a distance of 55 mm from the lens is shown in Fig. 4(b). The focal spot has an approximate diameter of 0.7 mm at FWHM. This compares favourably with the Abbe limit for the system of 0.6 mm and is a considerable improvement on the resolving power demonstrated by Ma [20]. All 12 lenses on the disk were characterised and it was found that the variation of focal point diameters and focal lengths is less than 5% of the design value.

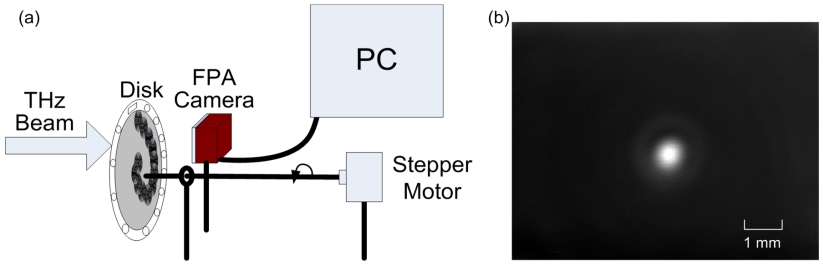


Fig. 4. (a) Illustration of the experimental setup for characterising the focal length and focal point of the lenses. (b) Image taken at the focal point of one of the 12 lenses.

#193636 - $15.00 USD Received 9 Jul 2013; revised 12 Sep 2013; accepted 24 Sep 2013; published 7 Oct 2013

## 3. Imaging system

The experimental setup of the imaging system is illustrated schematically in Fig. 5(a). The system consists of a CW THz source, a silicon Nipkow disk, a pyroelectric detecting system, and a PC-based Labview programme. The laser produced a Gaussian-like beam with a diameter of 16 mm and the CW THz signal had a maximum power of 150 mW. In order to rotate the silicon Nipkow disk and also establish the position of the lenses, a plastic disk holder, as shown in Fig. 5(b), was made. Experimental results show that the plastic holder has negligible transmission and low reflection, approximately 4.8% at the frequency of interest. There are three main sections on the disk holder. The outermost 11 circular holes and 1 rectangular hole were required for image synchronisation. A further twelve holes, of diameter 10 mm, were arranged spirally to allow the lens-focused beams to pass through and provide the Nipkow scan function of the disk. The terahertz beam is blocked by the plastic disk, except for where there are apertures. The innermost holes at the very centre were used for mounting the disk to an axis that was driven by a stepper motor [not shown in the Fig. 5(a)]. The silicon disk was glued on the plastic holder. The detecting system consists of a single pixel pyroelectric detector, a mechanical chopper, a lock-in amplifier (EG&G 5210) and an oscilloscope (Tektronics TPO 2400). A Labview programme was used to collect the data and construct the image. A piece of aluminum metal engraved with a "T" was made as the imaging object [see Fig. 6(a)]. The "T" had dimensions of 10 mm x10 mm.

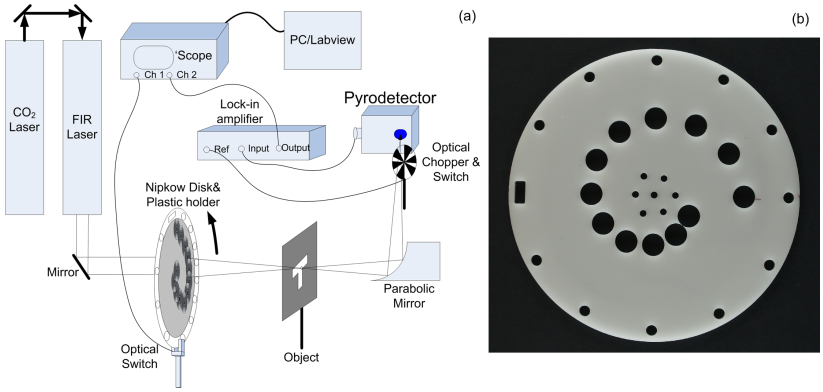


Fig. 5. (a) Illustration of the imaging system setup. (b) A plastic disk holder was made to accommodate the silicon Nipkow disk and is driven by a stepper motor.

The imaging process was as follows: the THz beam from the laser was incident on the disk and by rotating the disk at a constant speed of 3 rpm, each individual Fresnel lens, when in the beam, generated a focal point of 0.7 mm in diameter at a distance of 55 mm away from the disk. The 12 lenses formed an imaging plane. When placing the object "T" at the imaging plane, each focused beam behaved as a probe and scanned the object sequentially in both the x (radial) and y (rotational) directions. Figure 6(b) illustrates the imaging mechanism. Since each lens had a diameter of 10 mm which is 25 times greater area than a pinhole with a diameter of 2 mm according to Eq. (1), and taking into account the transmission of the silicon wafer which is 50% the total power at the focal point of a lens with an area of 2 mm in diameter is approximately 12 times greater than that of a pinhole with same size. The transmitted THz beams were collected by a parabolic mirror and then mechanically chopped before reaching the pyroelectric detector. The output signal of the pyroelectric detector was connected to the input of the lock-in amplifier. The mechanical chopper operated at a speed of 100 Hz which provided the reference signal to the lock-in amplifier. The output of the lock-in amplifier along with the timing signal from the plastic disk holder was then connected to two input channels of the oscilloscope. A computer was used to collect the data from the output of the oscilloscope and a Labview program was used to process the raw data and construct the image. An image with a pixel resolution of 2 mm in x direction as shown in Fig. 7(a) was

#193636 - $15.00 USD Received 9 Jul 2013; revised 12 Sep 2013; accepted 24 Sep 2013; published 7 Oct 2013

achieved with one revolution rotation of the disk. However, since each individual lens gave a focal spot of 0.7 mm in diameter that is much smaller than distance between the centres of two adjacent lenses in y direction which was 2 mm as devised, further improvement of image resolution was achieved using a multiframe technique as shown in Fig. 6(c) [25]. By applying 4 frames (the object "T" was shifted to the left 3 times in steps of 0.5 mm), an image with a pixel size of 0.5 mm was obtained and is shown in Fig. 7(b). As expected, because of the enhanced optical resolution obtained using a lens in place of a pinhole, the image is more uniform than was previously demonstrated using a conventional disk with the same pixel size. In addition, due to the smaller focal diameter at the imaging plane (0.7 mm compared to 2 mm in [20]), the system resolving power has also been improved. The resolution could be further improved by: increasing the numerical aperture of the lenses; increasing the number of frames in the multiframe method; or reducing the radial separation between lenses in order to increase the number of scanned lines. Slight distortion, which has been observed on Fig. 7(b), is mainly due to the movement of the object "T" as part of the multi-frame technique and power instability of the laser. This can be further improved by stabilising the laser, improving the system alignment, and applying an image averaging technique. The imaging speed was 3 frames per minute and this can be increased by spinning the disk faster and using a detector with a faster response.

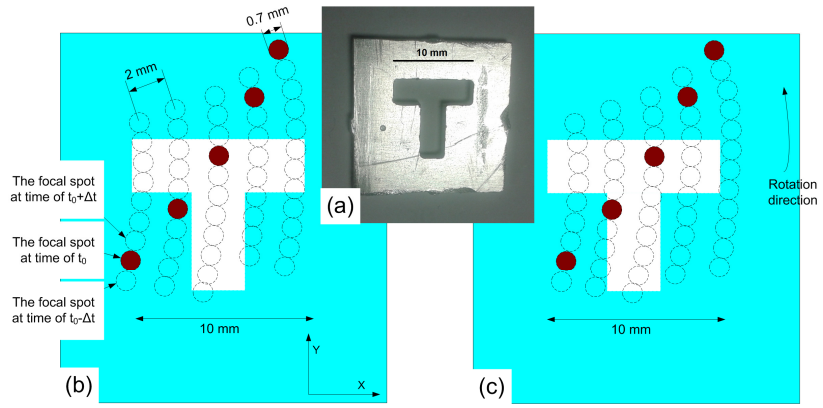


Fig. 6. (a) An optical image of the aluminium object "T" with dimensions of 10 mm x10 mm. (b) Illustration of the Nipkow imaging mechanism without using a multiframe technique and (c) the formation of the third fame of the image when the multiframe technique was used for improving the image resolution of (b). The object "T" in (c) was shifted to the left by 1 mm (2nd frame) from its original position.

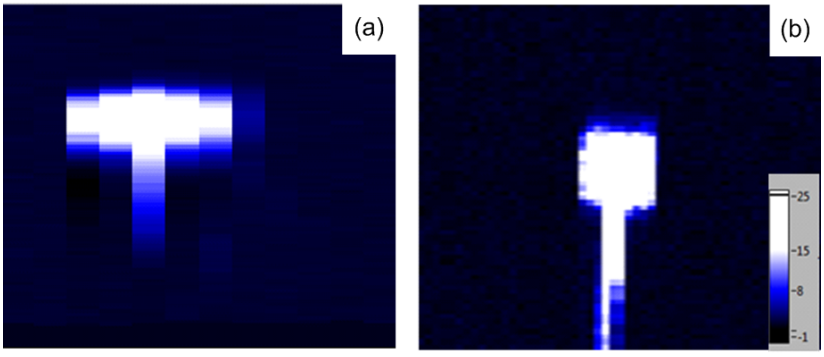


Fig. 7. The constructed 'T' images using the imaging system without (a) and with (b) using a multiframe technique. The pixel sizes in x-axial direction and the total numbers of pixel are 2 mm and 1200 for (a) and 0.5 mm and 4800 for (b), respectively.

#193636 - $15.00 USD Received 9 Jul 2013; revised 12 Sep 2013; accepted 24 Sep 2013; published 7 Oct 2013

## 4. Conclusions

We have demonstrated a novel design of a Nipkow disk for THz single pixel imaging systems with a high resolution. The disk is a 4" double-side polished high resistivity silicon wafer on which 12 Fresnel lenses were fabricated. The lenses have a diameter of 10 mm and focal length of 55 mm. The typical focal spots of the lenses have a diameter of 0.7 mm. An imaging system using such a disk has been demonstrated and an image with a resolution of 0.5 mm/pixel achieved. Further resolution improvements can be made by increasing the Fresnel lens numerical apertures and reducing radial separation or applying a multiframe technique.

#193636 - $15.00 USD Received 9 Jul 2013; revised 12 Sep 2013; accepted 24 Sep 2013; published 7 Oct 2013